

**Figure 1.** Top and side views of unit cells for each of the ten polymeric crystals studied in the present study. These include polyethylene (PE), polyacetylene (PA), poly(glycolic acid) (PGA), poly(phenylene oxide) (PPO), poly(oxymethylene) (POM), poly(*p*-phenylene sulfide) (PPS), two forms of poly(vinylidene fluoride) ( $\beta$ -PVDF and  $\delta$ -PVDF), poly(tetrafluoroethylene) (PTFE), and poly(vinyl chloride) (PVC). Gray, white, red, yellow, blue, and green spheres represent carbon, hydrogen, oxygen, sulfur, fluorine, and chlorine atoms, respectively. All unit cells are oriented such that the *c* lattice parameter always lies along the polymer chains.

The alternative DFT-D approach<sup>13,14</sup> is computationally just as demanding as DFT using (semi)local functionals as it includes the interatomic dispersion energy contributions to the DFT total energies as simple parametrized pairwise additive terms. A popular version of such a scheme is due to Grimme,<sup>13,14</sup> referred to here and in the literature as DFT-D2. It has been demonstrated that the computationally inexpensive DFT-D2 scheme yields reasonable predictions for the structure, bulk moduli, and cohesive energies of many weakly bonded materials for which DFT methods that use (semi)local functionals are inadequate.<sup>18</sup> However, the main drawback of the DFT-D2 approach is the high level of empiricism, requiring at least two fitting parameters for every element in the periodic table. Furthermore, different possible hybridization/oxidation states of atoms in different chemical or geometrical environments are not accounted for within the DFT-D2 scheme (as the same parameters are used for an element regardless of its environment).

Very recently, several groups have proposed different solutions to the above-mentioned issues.<sup>19–22</sup> Grimme et al.'s refined DFT-D3 method,<sup>22</sup> for instance, provides flexible and environment-dependent dispersion coefficients requiring only the structural (i.e., bond connectivity) information of the underlying system. This new D3 correction scheme represents a substantial improvement (in terms of accuracy, as well as appeal) over the previous D2 results for molecular systems and lattice constants of the bulk systems.<sup>13</sup> In addition, Tkatchenko

and Scheffler<sup>19</sup> have developed an alternative method (DFT-TS) to obtain the DFT-D parameters directly and self-consistently from the ground-state electron density, thereby incorporating the environment-dependence. The success of the DFT-TS scheme over conventional DFT and DFT-D2 has also been demonstrated for a variety of systems including polypeptide helices,<sup>23</sup> heterobilayers,<sup>24</sup> and adsorption on graphene.<sup>25</sup>

Though DFT-D approaches have proven to be accurate and necessary for a range of molecular systems, their predictive capability for polymeric crystals with different backbones and side chains is uncertain. In this paper, we consider 10 polymeric crystals (Figure 1) for which reliable crystallographic data is available. These include polyethylene (PE), polyacetylene (PA), poly(glycolic acid) (PGA), poly(phenylene oxide) (PPO), poly(oxymethylene) (POM), poly(*p*-phenylene sulfide) (PPS), two forms of poly(vinylidene fluoride) ( $\beta$ -PVDF and  $\delta$ -PVDF), poly(tetrafluoroethylene) (PTFE), and poly(vinyl chloride) (PVC). For these systems, we present a comparative assessment of the performance of the LDA, GGA, DFT-D2, DFT-D3 and DFT-TS functionals with respect to experiments. We find that although LDA and GGA lead to uniform and serious errors in the computed geometry and volume of the polymers considered (primarily due to the inaccurate determination of the lattice parameters controlled by interchain interactions), both the DFT-D3 and DFT-TS functionals provide results that are in favorable agreement with experiments. This work is expected to serve as a benchmark for future first-principles studies of the geometrical properties of polymers.

## THEORETICAL DETAILS

**Methodology and Computational Details.** The DFT calculations were carried out using the Vienna ab initio

**Table 1.** Plane Wave Energy Cutoffs ( $E_{\text{cut}}$ ) and Monkhorst–Pack *k*-Point Sampling Grids for Various Polymers Studied Here

polymer	$E_{\text{cut}}$ (eV)	<i>k</i> -point mesh
PE	800	4 × 4 × 10
PA	1000	6 × 3 × 10
PPO	800	3 × 5 × 3
POM	1000	5 × 3 × 5
PPS	800	3 × 5 × 3
PGA	1000	3 × 3 × 3
$\beta$ -PVDF	800	4 × 6 × 8
$\delta$ -PVDF	800	5 × 3 × 5
PTFE	1000	3 × 3 × 9
PVC	800	2 × 5 × 5

simulation package (VASP)<sup>26</sup> and the Fritz Haber Institute ab initio molecular simulations (FHI-aims)<sup>27</sup> codes. All VASP calculations utilized the projector-augmented wave (PAW) methodology.<sup>28,29</sup> The exchange–correlation functional used was either LDA or GGA [e.g., the Perdew–Burke–Ernzerhof (PBE) or Perdew–Wang 91 (PW91) functional].<sup>30</sup> The Grimme DFT-D2 or DFT-D3 method implemented in VASP was used, with the dispersion correction added to the DFT energy computed using the PBE functional. Henceforth we refer to this functional as PBE-D2 or PBE-D3, respectively. All DFT-TS calculations were performed using the FHI-aims code. PBE calculations were also performed using FHI-aims to ensure consistency of results between VASP and FHI-aims. For

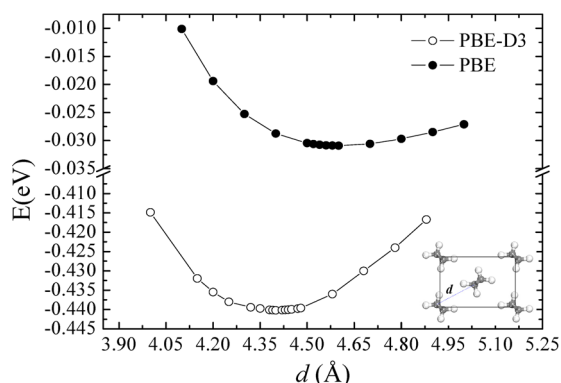


**Figure 2.** Cohesive energy versus the distance between polymer chains for PE computed with the PBE and PBE-D3 functionals.

instance, the lattice parameters of PE and PA computed with the PBE functional using FHI-aims varied by less than 0.5% with respect to the corresponding VASP results. The FHI-aims calculations employed a basis set of numerical atom-centered orbitals (NAO). The standard NAO basis set of tier2 for H, C, O, F and tier1 for S, Cl were used. Again, the dispersion corrections were added to the DFT energy computed using the PBE functional, and referred to as PBE-TS henceforth. Computational details such as plane wave cutoff ( $E_{\text{cut}}$ ) and Brillouin zone sampling for each system are summarized in Table 1.

For the polymeric crystals considered here, the Cartesian axes are chosen such that the  $a$  and  $b$  lattice parameters of all the systems lie along the directions normal to the polymer chains in a crystal and are thus determined by the interchain vdW interactions. On the other hand, the  $c$  lattice parameter is always taken along the chain direction, controlled by strong ionic-covalent interactions along the polymer backbone.

**Geometry Optimization.** It has now become a common practice to use automated schemes to perform geometry optimizations, including atomic and unit cell shape/size relaxations. These algorithms use predefined convergence criteria based on the magnitude of the energy differences between successive iterations, forces, or stresses. In the case of weakly bound systems, such automated approaches may not necessarily lead to the correct equilibrium ground state as the predefined convergence criteria may be met for geometries far

from the ground state (we note that further complications due to Pulay stresses<sup>31</sup> may arise in such automated geometry optimizations). To converge to the correct ground state, one may have to resort to tight convergence criteria that may not be practical. We use polyethylene (PE) as an example system to illustrate these challenges. Figure 2 shows the PBE and PBE-D3 total energies as a function of interchain distance; the latter was varied by scaling the  $a$  and  $b$  lattice parameters of this system. The rather shallow minimum predicted by the PBE functional (compared to the PBE-D3 case) is indicative of the challenges an automated optimizer would face in locating this minimum. Not surprisingly, automatic geometry optimizations starting from different initial geometries and using even very tight convergence criteria ( $10^{-6}$  eV for the energy and  $10^{-2}$  eV/Å for the atomic forces) lead to wildly different converged final lattice parameters when the PBE functional was used. The issue was alleviated in the case of the other functionals as the potential energy surface close the minimum was not as shallow as for the PBE functional. Thus, particular care must be taken in determining the equilibrium geometry using automated approaches.

An alternative, more reliable way to avoid artifacts related to the Pulay stresses and shallow potential energy surfaces is to perform a scan of the potential energy surface (Figure 3). Here, we performed such a study by varying both  $a$  and  $b$  lattice parameters independently over a broad range of values; the  $c$  lattice parameter (along the chain axis) was determined first for an isolated chain and held fixed at this value while  $a$  and  $b$  were varied. For each choice of  $a$ ,  $b$ , and  $c$ , the atomic coordinates were allowed to relax until the total energy and the total force were converged to better than  $10^{-6}$  eV and  $10^{-2}$  eV/Å, respectively. Although time-intensive, we find that this approach provides the most reliable determination of the lattice parameters and geometry (at a given level of theory) for all systems considered. Thus, our results reported in the next section were all obtained using this strategy.

## RESULTS AND DISCUSSIONS

For the ten polymers considered, Figure 3 shows the cohesive energy contour plots computed at the PBE-TS level of theory as a function of the lattice parameters  $a$  and  $b$ . The equilibrium lattice parameters obtained from LDA, PBE, PBE-D2, and PBE-D3 functionals as well as the experimental values are also

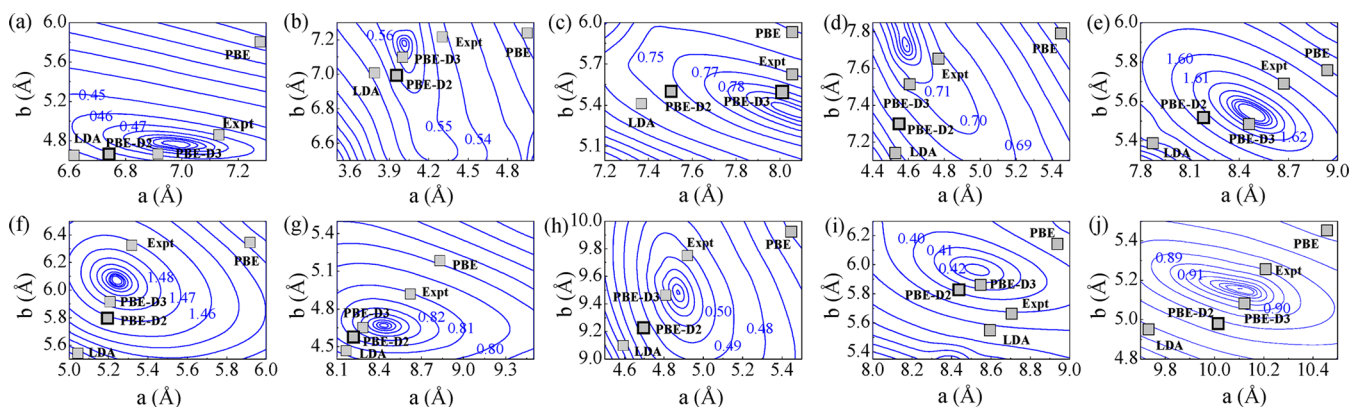


**Figure 3.** Cohesive-energy (eV) as a function of the lattice parameters  $a$  and  $b$  of (a) PE, (b) PA, (c) PPO, (d) POM, (e) PPS, (f) PGA, (g) PVDF ( $\beta$ ), (h) PVDF ( $\delta$ ), (i) PTFE, and (j) PVC, computed at the PBE-TS (blue, solid line) level of theory. The equilibrium lattice parameters obtained from PBE-D2, PBE-D3, PBE, and LDA functionals in the present study as well as those from experimental studies are also shown for comparison. For clarity, the PW91 results are not shown as they are, in general, very close to the PBE results.

**Table 2. Computed and Experimental Lattice Parameters, Densities, Cohesive Energies ( $E_c$ ), and Bulk Moduli ( $B_0$ ) for PE, PA, PPO, POM, PPS, PGA,  $\beta$ -PVDF,  $\delta$ -PVDF, PTFE, and PVC Crystals**

polymer	method	$a$ (Å)	$b$ (Å)	$c$ (Å)	density (g/cm <sup>3</sup> )	$E_c$ (eV)	$B_0$ (GPa)	polymer	method	$a$ (Å)	$b$ (Å)	$c$ (Å)	density (g/cm <sup>3</sup> )	$E_c$ (eV)	$B_0$ (GPa)
PE ( <i>Pnma</i> )	expt <sup>17</sup>	7.12	4.85	2.55	0.997	0.40	5.6	PGA ( <i>Pcmm</i> )	expt <sup>34</sup>	5.22	6.19	7.02	1.700		
	LDA	6.60	4.45	2.52	1.259	0.44	23.9		LDA	5.07	5.58	6.96	1.958	1.73	10.2
	PBE	8.20	5.60	2.55	0.796	0.03	16.4		PBE	5.86	6.31	7.06	1.477	0.51	3.2
	PW91	8.13	5.64	2.55	0.797	0.04	15.7		PW91	5.91	6.25	7.06	1.479	0.55	3.5
	PBE-D2	6.66	4.56	2.55	1.203	0.44	19.7		PBE-D2	5.22	5.89	7.04	1.781	1.48	9.2
	PBE-D3	6.95	4.72	2.55	1.114	0.44	19.8		PBE-D3	5.20	6.06	7.04	1.738	1.45	8.8
	PBE-TS	7.01	4.76	2.56	1.091	0.52	21.4		PBE-TS	5.09	6.11	7.03	1.763	1.55	9.4
	expt <sup>32</sup>	4.24	7.32	2.46	1.130				$\beta$ -PVDF ( <i>Cm2m</i> )	expt <sup>32</sup>	8.58	4.91	2.56	1.972	
PA ( $P2_1/n$ )	LDA	3.82	7.00	2.45	1.320	0.72	13.1	LDA	7.99	4.49	2.54	2.334	0.74	34.9	
	PBE	5.00	7.74	2.46	0.908	0.05	2.8	PBE	8.90	5.07	2.58	1.827	0.38	10.5	
	PW91	5.08	7.69	2.46	0.899	0.06	3.6	PW91	8.97	4.95	2.58	1.857	0.41	9.7	
	PBE-D2	3.82	7.02	2.46	1.311	0.53	9.9	PBE-D2	8.28	4.58	2.57	2.182	0.86	25.1	
	PBE-D3	3.96	7.11	2.46	1.248	0.55	10.1	PBE-D3	8.30	4.68	2.57	2.131	0.83	24.3	
	PBE-TS	4.01	7.19	2.46	1.219	0.60	10.7	PBE-TS	8.29	4.70	2.57	2.124	0.87	30.6	
	expt <sup>32</sup>	8.07	5.54	9.72	1.408		4.1	$\delta$ -PVDF ( $P2_1/c$ )	expt <sup>32</sup>	9.64	4.96	4.62	1.925		
	LDA	7.31	5.51	9.78	1.553	1.90	11.6	LDA	9.03	4.56	4.62	2.235	0.32	24.1	
PPO ( <i>Pbcn</i> )	PBE	8.42	5.88	9.85	1.254	0.22	4.4	PBE	10.35	5.17	4.64	1.712	0.15	8.3	
	PW91	8.38	5.78	9.85	1.281	0.25	4.9	PW91	10.37	5.08	4.64	1.739	0.17	8.5	
	PBE-D2	7.55	5.51	9.79	1.502	1.75	10.6	PBE-D2	9.33	4.72	4.63	2.085	0.55	15.1	
	PBE-D3	8.00	5.50	9.77	1.423	1.72	10.3	PBE-D3	9.46	4.82	4.63	2.013	0.52	15.4	
	PBE-TS	8.04	5.37	9.75	1.453	1.82	11.8	PBE-TS	9.48	4.87	4.63	1.989	0.58	21.6	
	expt <sup>32</sup>	4.77	7.65	3.56	0.922			PTFE ( <i>Pnma</i> )	expt <sup>35</sup>	8.73	5.69	2.62	2.552		
	LDA	4.50	7.04	3.50	1.080	0.75	20.2	LDA	8.63	5.64	2.59	2.635	0.24	15.5	
	PBE	5.40	8.37	3.63	0.730	0.17	3.9	PBE	8.98	6.16	2.65	2.266	0.12	4.2	
POM ( $P2_12_12_1$ )	PW91	5.36	8.26	3.63	0.745	0.19	5.1	PW91	8.92	6.18	2.65	2.274	0.16	4.9	
	PBE-D2	4.57	7.36	3.58	0.994	0.70	15.6	PBE-D2	8.42	5.91	2.65	2.519	0.40	9.0	
	PBE-D3	4.60	7.53	3.58	0.966	0.70	15.9	PBE-D3	8.55	5.85	2.64	2.516	0.42	9.2	
	PBE-TS	4.59	7.72	3.57	0.947	0.76	16.6	PBE-TS	8.53	5.97	2.63	2.480	0.44	11.2	
	expt <sup>32</sup>	8.67	5.61	10.26	1.440			PVC ( <i>Pbcn</i> )	expt <sup>32</sup>	10.24	5.24	5.08	1.523		6.0
	LDA	7.80	5.44	10.23	1.655	1.80	12.5	LDA	9.42	5.00	5.04	1.749	1.00	14.9	
	PBE	8.85	5.73	10.26	1.381	0.12	3.4	PBE	10.45	5.50	5.05	1.430	0.21	2.5	
	PW91	8.92	5.76	10.26	1.363	0.16	4.3	PW91	10.52	5.56	5.05	1.405	0.25	3.1	
PPS ( <i>Pbcn</i> )	PBE-D2	8.20	5.51	10.25	1.551	1.55	9.7	PBE-D2	10.05	5.07	5.10	1.598	0.90	7.9	
	PBE-D3	8.42	5.52	10.25	1.508	1.52	10.0	PBE-D3	10.13	5.12	5.08	1.575	0.87	8.2	
	PBE-TS	8.48	5.54	10.25	1.492	1.69	10.7	PBE-TS	10.11	5.15	5.08	1.570	0.95	8.8	

shown for comparison in each of the panels. The cohesive energy ( $E_c$ ) per monomer unit has been calculated using the following equation

$$E_c = \frac{N_{\text{chain}}E_{\text{chain}} - E_{\text{bulk}}}{N_{\text{units}}} \quad (1)$$

where  $E_{\text{bulk}}$  and  $E_{\text{chain}}$  are the total energies of the bulk unit cell and of the single isolated polymer chain, respectively, and  $N_{\text{chain}}$  and  $N_{\text{units}}$  are the total number of polymer chains and the number of monomer units forming the bulk unit cell, respectively.  $E_{\text{chain}}$  was calculated for sufficiently large

simulation cells to eliminate spurious interactions between neighboring chains.

The actual value of the lattice parameters, densities, cohesive energies, and bulk moduli for the ten polymeric crystals calculated using different functionals at their respective optimized geometries are presented in Table 2. The bulk moduli were computed using a procedure appropriate for highly anisotropic systems<sup>36</sup> such as the polymers considered here.

Overall, we find that our results are comparable with previously reported theoretical results in the literature (cf. Table 2). Barone et al.<sup>11</sup> have computed values of  $(a, b) = (6.67$

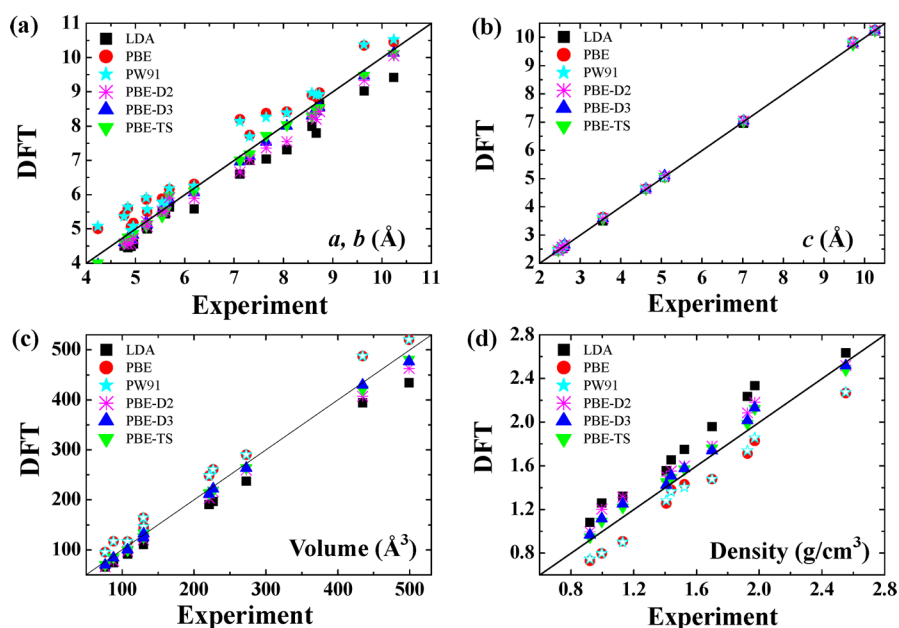


**Figure 4.** Comparison between the computed and the corresponding experimental values of lattice parameters (panels a and b) and volumes (c) and densities (d) for the ten polymers studied here using different functionals.

**Table 3. Root-Mean-Square Error of the Lattice Parameters (*a* and *b*) and Volume of the Ten Polymeric Crystals Studied for Various Levels of Theory**

functional	<i>a</i> , <i>b</i> (Å)	volume (Å <sup>3</sup> )
LDA	0.47	25.75
PBE	0.52	30.84
PW91	0.50	27.03
PBE-D2	0.29	13.77
PBE-D3	0.23	9.53
PBE-TS	0.19	8.93

Å, 4.55 Å), and  $E_c = 0.41$  eV for PE using the PBE-D2 method. We note though that the PBE-D3 method yields more accurate predictions of the geometry for PE. Recently, nonlocal vdW-DF<sup>15</sup> has also been used to determine the crystal structure and the cohesive energy of PE. The computed values (*a*, *b*) = (7.30 Å, 5.22 Å), are larger than those obtained from the PBE-D3 scheme and experiments. For PA, Zicovich-Wilson et al.<sup>37</sup> have reported that the B3LYP hybrid functional strongly overestimates the lattice parameters (*a*, *b*) = (6.521 Å, 8.555 Å), whereas B3LYP-D with Grimme's correction improves the agreement with the experimental values (*a*, *b*) = (3.982 Å, 7.408 Å).

From Figure 3 and Table 2, we find that conventional electron exchange–correlation functionals (e.g., LDA, PBE, PW91) are, in general, unable to correctly capture the structural parameters governed by secondary bonding. The calculated structural results are compared against the respective experimental values as parity plots in Figure 4. As shown in panels a and b, whereas all the functionals show a very good agreement for the *c* lattice parameters for different polymers, the calculated *a* and *b* lattice parameters show a significant scatter with respect to the corresponding experimental values. As a general feature, we find that the LDA and PBE (or PW91) functionals, respectively, underestimate and overestimate both the *a* and *b* lattice parameters and consequently result in errors

in the computed volume and density, as depicted in Figures 4c and 4d.

The dispersion-corrected functionals, on the other hand, significantly improve the description of the lattice parameters with respect to the LDA, PBE and PW91 functionals, as is evident from Figure 3, Figure 4, and Table 2. To further quantify the performance of the considered functionals in predicting the structural parameters (*a* and *b*) and equilibrium crystal volume, we calculated the root-mean-square error (RMSE) with respect to the available experimental values. Our results are presented in Table 3. We find that the PBE-D2 scheme, despite the usage of fixed dispersion coefficients already constitutes a significant improvement over the (semi)-local functionals. The more flexible and environment-dependent dispersion coefficients afforded by the PBE-D3 and PBE-TS schemes lead to further improvements in the fidelity of the structural predictions, with these two schemes being roughly equivalent in terms of the quality of their predictions. The residual differences between the PBE-D3 and PBE-TS results may be accounted for by the differences in the two schemes, and also, partly due to small basis set superposition errors inherent in the FHI-aims implementation used in the PBE-TS calculations.

The calculated cohesive energies and bulk moduli at various levels of theory for the ten polymers are also reported in Table 2. As a general trend, LDA (PBE or PW91) cohesive energies and bulk moduli are always on the higher (lower) side of the spectrum of the calculated values for a given polymer. These predictions are consistent with the well-known notions of the tendency of LDA (PBE or PW91) to overbind (underbind), also reflected in our predicted lattice parameters. In general, the PBE-TS functional always predicts slightly higher cohesive energies and bulk moduli as compared to those predicted by the PBE-D3. These findings are consistent with the previously known overestimation of the interlayer binding energy in graphite by the PBE-TS functional.<sup>38</sup>

## SUMMARY

We have systematically tested the performance of conventional (semi)local electron exchange–correlation functionals (e.g., LDA, PBE, and PW91) and dispersion-corrected functionals (e.g., PBE-D2, PBE-D3, and PBE-TS) for a variety of representative polymer systems. Our calculations show that the (semi)local functionals do not provide an adequate description of the polymer interchain interactions which are dominated by van der Waals interactions, and consequently lead to inaccuracies in the computed geometries and cohesive properties. The dispersion-corrected functionals, on the other hand, especially PBE-D3 and PBE-TS (which contain environment-dependent dispersion coefficients), result in improved predictions of the structural and energetic properties, and possibly, the elastic properties as well. We do note though that the PBE-D2 scheme, which includes fixed (environment-independent) dispersion coefficients already leads to significant improvements in the predictions of structural properties of polymers with respect to the purely (semi)local functionals. The present work is expected to serve as a benchmark for future first-principles studies of the structural properties of polymers.

## AUTHOR INFORMATION

### Corresponding Author

\*E-mail: rampi@uconn.edu.

### Notes

The authors declare no competing financial interest.

## ACKNOWLEDGMENTS

This paper is based upon work supported by a multidisciplinary university research initiative (MURI) grant from the Office of Naval Research. Computational support was provided through a National Science Foundation Teragrid Resource Allocation. R.R. thanks Matthias Scheffler (Fritz-Haber-Institut) for graciously sharing the FHI-aims code. C.S.L. thanks Stefan Grimme (U. Münster) for providing the DFT-D3 code and Y. Li for help with the DFT-D3 calculations. Helpful discussions and interactions with Kenneth Jordan (University of Pittsburgh), Alexandre Tkatchenko (Fritz-Haber-Institut), and Mina Yoon (Oak Ridge National Laboratories) are also acknowledged.

## REFERENCES

- (1) Ouyang, J.; Chu, C. W.; Szmanda, C. R.; Ma, L. P.; Yang, Y. *Nat. Mater.* **2004**, *3*, 918–922.
- (2) Nie, Z. H.; Kumacheva, E. *Nat. Mater.* **2008**, *7*, 277–290.
- (3) Tomer, V.; Polizos, G.; Randall, C. A.; Manias, E. *J. Appl. Phys.* **2011**, *109*, No. 074113.
- (4) Simon, P.; Gogotsi, Y. *Nat. Mater.* **2008**, *7*, 854.
- (5) Kleis, J.; Schröder, E. *J. Chem. Phys.* **2005**, *122*, No. 164902.
- (6) Heeger, A. J. *Rev. Mod. Phys.* **2001**, *73*, 681–700.
- (7) Park, D. H.; Kim, M. S.; Joo, J. *J. Chem. Soc. Rev.* **2010**, *39*, 2439–2452.
- (8) Roberts, M.; Queralto, N.; Mannsfeld, S. C. B.; Reinecke, B. N.; Knoll, W.; Bao, Z. *Chem. Mater.* **2009**, *21*, 2292–2299.
- (9) Martin, R. M. *Electronic Structure: Basic Theory and Practical Methods: Basic Theory and Practical Density Functional Approaches*; Cambridge University: Cambridge, U.K.; Vol. 1.
- (10) Langreth, D. C.; Lundqvist, B. I.; Chakarova-Käck, S. D.; Cooper, V. R.; Dion, M.; Hyldgaard, P.; Kelkkanen, A.; Kleis, J.; Kong, L.; Li, S.; Moses, P. G.; Murray, E.; Puzder, A.; Rydberg, H.; Schröder, E.; Thonhauser, T. *J. Phys.: Condens. Matter* **2009**, *21*, 084203–084217.

- (11) Barone, V.; Casarin, M.; Forrer, D.; Pavone, M.; Sambri, M.; Vittadini, A. *J. Comput. Chem.* **2009**, *30*, 934–939.
- (12) Dion, M.; Rydberg, H.; Schröder, E.; Langreth, D. C.; Lundqvist, B. I. *Phys. Rev. Lett.* **2004**, *92*, No. 246401.
- (13) Grimme, S. *WIREs Comput. Mol. Sci.* **2001**, *1*, 211. Ehrlich, S.; Moellmann, J.; Reckien, W.; Bredow, T.; Grimme, S. *Chem. Phys. Chem.* **2011**, *12*, 3414–3420.
- (14) Grimme, S. *J. Comput. Chem.* **2006**, *27*, 1787–1799.
- (15) Kleis, J.; Lundqvist, B. I.; Langreth, D. C.; Schröder, E. *Phys. Rev. B* **2007**, *76*, No. 100201.
- (16) Chakarova-Käck, S. D.; Schröder, E.; Lundqvist, B. I.; Langreth, D. C. *Phys. Rev. Lett.* **2006**, *96*, No. 146107. Chakarova-Käck, S. D.; Borck, Å.; Schröder, E.; Lundqvist, B. I. *Phys. Rev. B* **2006**, *74*, No. 155402.
- (17) Avitabile, G.; Napolitano, R.; Pirozzi, B.; Rouse, K. D.; Thomas, M. W. *J. Polym. Sci. Polym. Lett. Ed.* **1975**, *13*, 351–355.
- (18) Bučko, T.; Hafner, J.; Lebègue, S.; Ángyán, J. G. *J. Phys. Chem. A* **2010**, *114*, 11814–11824.
- (19) Tkatchenko, A.; Scheffler, M. *Phys. Rev. Lett.* **2009**, *102*, No. 073005.
- (20) Johnson, E. R.; Becke, A. D. *J. Chem. Phys.* **2005**, *123*, No. 024101.
- (21) Silvestrelli, P. L. *Phys. Rev. Lett.* **2008**, *100*, No. 053002.
- (22) Grimme, S.; Antony, J.; Ehrlich, S.; Krieg, H. *J. Chem. Phys.* **2010**, *132*, No. 154104.
- (23) Tkatchenko, A.; Rossi, M.; Blum, V.; Ireta, J.; Scheffler, M. *Phys. Rev. Lett.* **2011**, *106*, No. 118102.
- (24) Fan, Y.; Zhao, M.; Wang, Z.; Zhang, X.; Zhang, H. *Appl. Phys. Lett.* **2011**, *98*, No. 083103.
- (25) Björk, J.; Hanke, F.; Palma, C.; Samori, P.; Cecchini, M.; Persson, M. *J. Phys. Chem. Lett.* **2010**, *1*, 3407–3412.
- (26) Kresse, G.; Furthmüller, J. *Phys. Rev. B* **1996**, *54*, No. 11169.
- (27) Blum, V.; Gehrke, R.; Hanke, F.; Havu, P.; Havu, V.; Ren, X.; Reuter, K.; Scheffler, M. *Comput. Phys. Commun.* **2009**, *180*, 2175–2196.
- (28) Blochl, P. E. *Phys. Rev. B* **1994**, *50*, No. 17953.
- (29) Kresse, G.; Joubert, D. *Phys. Rev. B* **1999**, *59*, No. 1758.
- (30) Perdew, J. P.; Burke, K.; Ernzerhof, M. *Phys. Rev. Lett.* **1996**, *77*, No. 3865.
- (31) Francis, G. P.; Payne, M. C. *J. Phys.: Condens. Matter.* **1990**, *2*, 4395–4404.
- (32) Miller, R. L. Crystallographic data and melting points for various polymers. In *Polymer handbook. Part VI: Solid state properties*. 4th revised ed.; Brandrup, J., Immergut, E. H., Grulke, E. A., Abe, A., Bloch, D. R., Eds.; Wiley: New York, 1999; Electronic Ed. 2005; ISBN 1-59124-883-3.
- (33) Carazzolo, G.; Mammi, M. *J. Polym. Sci.* **1963**, *1*, 965–983.
- (34) Chatani, Y.; Suehiro, K.; Okita, Y.; Tadokoro, H.; Chujo, K. *Makromol. Chem.* **1968**, *113*, 215–229.
- (35) Nakafuku, C.; Takemura, T. *Jpn. J. Appl. Phys.* **1975**, *14*, 599–602.
- (36) Kim, E.; Chen, C. *Phys. Lett. A* **2004**, *326*, 442–448.
- (37) Zicovich-Wilson, C. M.; Kirtman, B.; Civalleri, B.; Ramirez-Solis, A. *Phys. Chem. Chem. Phys.* **2010**, *12*, 3289–3293.
- (38) Park, J.; Yu, B. D.; Hong, S. *J. Korean Phys. Soc.* **2011**, *59*, 196–199.

## Correction to “How Critical Are the van der Waals Interactions in Polymer Crystals?”

Chun-Sheng Liu, Ghanshyam Pilania, Chenchen Wang, and Ramamurthy Ramprasad\*

*J. Phys. Chem. A* **2012**, *116* (37), 9347–9352. DOI: 10.1021/jp3005844

In Figure 1, PVDF( $\delta$ ) should be PVDF( $\alpha$ ). In Table 1 and the text,  $\delta$ -PVDF should be  $\alpha$ -PVDF. In Table 2, the LDA calculated lattice parameters ( $a$  and  $b$ ) and density are incorrect for PE. The correct results should be  $a = 6.68 \text{ \AA}$ ,  $b = 4.59 \text{ \AA}$ , and density =  $1.206 \text{ g/cm}^3$ . Also in Table 2,  $\delta$ -PVDF should be  $\alpha$ -PVDF. The cohesive energy in Table 2 is per unit cell, not per monomer as shown in eq 1. Therefore, the text on p 9350 should read “The cohesive energy ( $E_c$ ) per unit cell has been calculated using the following equation”

$$E_c = N_{\text{chain}}E_{\text{chain}} - E_{\text{bulk}} \quad (1)$$

### ■ ACKNOWLEDGMENTS

The authors want to thank Dr. Nguyen Huy Viet and Dr. Thinkh Pham for pointing out some of the errors in the original paper.